Probing a dielectric resonator acting as passive sensor through a wireless microwave link

J.-M Friedt,[1, a)] R. Boudot,[2] G. Martin,[2] and S. Ballandras[3]

[1)] *SENSeOR SAS, c/o FEMTO-ST time & frequency, Besançon, France*

[2)] *FEMTO-ST, Time & frequency department, UMR CNRS 6174, Univ. Franche Comté, Besançon, France*

[3)] *Frec'n'sys, Besançon, France*

(Dated: 25 July 2014)

Dielectric resonators, generally used for frequency filtering in oscillator loops, can be used as passive cooperative targets for wireless sensor applications. In the present work, we demonstrate such an approach by probing their spectral characteristics using a microwave RADAR system. The unique spectral response and energy storage capability of resonators provide unique responses allowing to separate the sensor response from clutter. Although the dielectric resonator is not designed for high temperature sensitivity, the accurate determination of the resonance frequency allows for a remote estimate of the temperature with kelvin resolution.

PACS numbers: 84.40.-x,43.20.Ye, 43.38.Rh

Keywords: wireless, battery-less, sensor, dielectric resonator, RADAR

[a)] Electronic mail: jmfriedt@femto-st.fr; http://jmfriedt.free.fr

I. INTRODUCTION

A sensor consists of a sensing element – a transducer converting the physical quantity under investigation, to a usable quantity – and a signal shaping circuit. Although these two elements are classically linked by electrical wires (e.g. resistive probe and Wheatstone bridge), intrinsically radiofrequency transducers allow for a wireless, radiofrequency link between the sensing element and the signal processing circuit which is then acting similarly to a RADAR system[1].

Acoustic transducers based on a piezoelectric substrate which converts incoming electromagnetic energy to an acoustic wave confined to the substrate surface have been the topic of intense investigation[2–7]. Such systems exploit the acoustic wave velocity dependence with the physical quantity under investigation. This sensitivity is tuned by selecting an appropriate piezoelectric substrate orientation. The direct piezoelectric effect then converts back the acoustic energy to an electromagnetic signal detected by the RADAR receiver. Surface acoustic transducer operating frequency is limited to about 6 GHz by technological challenges[8] (clean-room lithography resolution) and intrinsic acoustic losses[9].

An alternative to acoustic transducers when aiming for microwave frequencies is the use of dielectric resonators[10–13]. While dielectric resonator dimensions make them hardly usable in the radiofrequency range, a 10 GHz dielectric resonator is in the 5-mm diameter range, well within the acceptable transducer size in industrial maintenance applications. Most significantly, operating above 10 GHz (3 cm wavelength or 0.75 cm quarter-wavelength) allows for compact antennas so that the whole sensing system made of the sensing element *and the associated antenna* remains compact. On the interrogating RADAR side, microwave frequencies allow for the deployment of antenna arrays even in the space-constrained environments met in industrial machinery (e.g. motors). Rising the operating frequency is of interest to provide the means for advanced signal processing techniques such as beam steering for sensor identification through Space-Division Multiple Access (SDMA). Such strategies are hardly applicable in practical environments even in the 2.45 GHz Industrial, Scientific and Medical (ISM) band currently used for acoustic sensor interrogation[14].

In this presentation, we demonstrate the wireless measurement of the resonance frequency of a dielectric resonator for a sensing application. The resonance frequency remains stable despite radiofrequency propagation channel disturbances[15]. At the opposite, previous in-

vestigations focused on analyzing the RADAR cross-section (magnitude measurement as a function of frequency)[16–20]. The drawback of the latter approach is its strong sensitivity to environment variations, since the RADAR cross section is not only dependent on the signal returned by the sensing element but also by the propagation channel. Energy storage in the resonator and slow release provide a unique signature of the sensing element with respect to the surrounding broadband passive reflectors generating unwanted clutter. By selecting measurement parameters in which clutter has faded out and only the resonator signal remains, an appropriate signal-to-noise ratio for multiple-meter measurement range is demonstrated, thus resulting in *far-field interrogation* conditions.

II. BASICS

The most common architecture for microwave RADAR systems is the classical frequency-modulated continuous wave (FMCW) approach in which a tunable local oscillator (LO) generates a linearly varying continuous wave. Part of the energy feeds an antenna while the other part reaches a mixer: as the electromagnetic wave emitted at time t and frequency $f(t)$ propagates to reach a target during a two-way trip duration τ, the sweeping LO frequency has moved to a new frequency $f(t+\tau)$. Mixing these two waves yields a beat signal of frequency $f(t+\tau) - f(t)$, which, assuming a linear evolution of f, is only dependent on the time interval τ whatever the initial $f(t)$. The linearity of the LO is a significant challenge for a coherent accumulation of the beat signal during the Fourier transform process to convert the beat signal to a range information in classical FMCW. This issue is not met when probing a dielectric resonator with a frequency swept signal in an FMCW architecture: the beat signal is only locally generated when $f(t)$ reaches the resonance frequency of the resonator. The mixing process aims at converting the microwave signal, which cannot be processed by digital means using current technology constraints, to an audiofrequency beat signal for digital processing aimed at identifying the resonance frequency. The beat signal frequency itself is not used for this identification process, only the fact that the resonator has stored energy and released it during a time constant Q/π periods after the excitation has ended[21]. Using typical values of dielectric resonator characteristics[22], the quality factor $Q = 10^4$ of a resonator operating in the $f_0 \simeq 10$ GHz range yields a time constant $\tau = \frac{Q}{\pi f_0} \simeq 320$ ns. Such a delay would be associated with a target located, assuming a two-way trip delay in

vacuum of the electromagnetic wave, at 50 m. Such a range is not accessible to short-range RADAR systems[23] designed to probe a sensing element only a few meters away. Thanks to the low requirements on the local oscillator linearity, an open-loop voltage controlled oscillator (VCO) monitored by a linearly varying voltage will be used as the LO generator.

Reaching the microwave domain means that the antenna is no longer limited to the few very basic schemes accessible in the radiofrequency range (dipole, monopole, possibly PIFA[24] if the allocated space constraint allow for such configurations) but highly efficient architectures can be considered, even parabola with gains hardly accessible in the radiofrequency range. Thus, the poor coupling between the antenna and the dielectric resonator – a key aspect of the efficient remote interrogation of the sensing element – is partly compensated for by the improved antenna gain.

III. EXPERIMENTAL DEMONSTRATION

The transfer function of the dielectric resonator used in this experiment is shown in Fig.1. Undercoupling is visible on the phase diagram. A loaded quality factor (width of the resonance at 3 dB from the baseline) of 3800 is observed, which yields an unloaded quality factor of 5300 considering the $\min(|S_{11}|) = -7.2$ dB. This poor matching is representative of the variable link budget met in practical applications. Providing a robust means of coupling the dielectric resonator to the antenna, compatible with the space constraint of a compact sensing element, remains an open challenge. In our case, the coupling is provided by a magnetic loop antenna located close to the dielectric resonator in an electromagnetic cavity.

[FIG. 1 about here.]

The basic scheme of the microwave interrogation strategy is based on the FMCW RADAR setup, with no VCO linearization strategy (Fig. 2). The link budget estimate includes the antenna gain, the Free Space Propagation Loss (FSPL, -105 dB at a distance of 1 m at 10 GHz) and neglects the strongly coupled resonator losses. The link budget yields a received power close to those found in the reader developed for interrogating 434 MHz acoustic resonators[25]. Notice that no dedicated amplification circuit was added on the microwave reception branch nor after the radiofrequency amplifier located at the mixer output.

[FIG. 2 about here.]

The frequency sweep of the LO is controlled by a triangle shaped drive voltage ranging from 2.0 to 2.2 V at a frequency of 5 kHz (Fig. 3, bottom). Since the associated Hittite HMC512 VCO output frequency has been measured to be in the 9.817857 to 9.860508 GHz range, the frequency sweep rate is 42.6 MHz during 100 μs or 426 kHz/μs. Considering an energy storage time constant of the resonator of $Q/(\pi f_0) = 320$ ns, the expected beat signal (Fig. 3, top) frequency is $426 \times 0.32 \simeq 140$ kHz, or a returned signal with $1/0.14 \simeq 7$ μs period. Such a signal is indeed observed at the output of the mixer close to the resonance frequency of the dielectric resonator, for different resonator temperatures (Fig. 3, top).

[FIG. 3 about here.]

In order to identify accurately the resonance frequency as the position of maximum of the returned signal, we use the zero-crossing condition of the derivate of the beat signal (Fig. 4, top). In our experiment, we worked using only the I-component of the returned signal. The drawback of this approach is to induce a dependence of the signal with distance (phase). A better method would be to process the full I/Q components for a robust signal processing approach.

Fig. 4 (bottom) shows the resonator relative frequency (left axis) and associated temperature error (right axis) versus temperature. The resulting slope of the relative frequency curve provides a first order temperature coefficient of frequency TCF_1 of about 20 ppm/K. This value is well higher than typical values reported in the literature and most datasheets, but below the value of 100 ppm/K reported in[26]. A large temperature sensitivity is required for temperature sensing applications. If considering a temperature measurement range of 0 to 250^{o}C and targeting the 250 MHz wide unregulated band starting at 24 GHz, compliance with the radiofrequency emission regulations requires a TCF_1 value below $\frac{250 \cdot 10^6}{250} \times \frac{1}{24 \cdot 10^9} \simeq 42$ ppm/K. The temperature resolution, shown on Fig. 4 (bottom, right axis), is 3 K as found as the standard deviation of the subtracted temperature estimate from the nominal outer dielectric resonator cavity temperature. The actual dielectric resonator temperature itself cannot be measured since no temperature probe is located inside the cavity.

[FIG. 4 about here.]

IV. DISCUSSION

All experiments were performed by holding a dielectric resonator inside a high-quality cavity and coupling the electromagnetic field with a loop antenna. Such a cumbersome approach is hardly applicable for a compact passive sensor, yet provides an excellent quality factor. We have observed on the cavity port quality factors ranging from 2100 to 6000±1000 as the insertion losses at the minimum of the reflection coefficient magnitude is tuned from -25 dB (near critical coupling) to -5 dB. In all cases, the signal was well identified using the setup described in the experimental section. However, replacing the metallic cavity by a microstrip coupling[27] drops the quality factor to below 150, due to the electromagnetic leakage losses. Such a condition does not allow for the distinction of the sensor signal and extraction from the background clutter. Similarly, spanning too wide a frequency range (>50 MHz at 9.8 GHz) yields beat signals from wideband reflectors which hide the targeted resonator signal. Hence, *proper packaging of the dielectric resonator is a mandatory condition for far field wireless interrogation* and a simple microstrip coupler in air does not allow for a sufficient quality factor for wireless sensing.

A second issue is the monomode resonance provided by the $TE_{01\delta}$ electrical energy distribution in the resonator. A single resonance does not allow for a referenced measurement, mandatory for a precise and accurate physical quantity identification immune to distance variation from the reader unit to the cooperative target on the one hand, and to local oscillator drift on the other hand. Either multimode transducers[28] or closely spaced modes are required for such an approach. Whispering Gallery Modes (WGM) have been classically selected for their strong confinement in the dielectric resonator and hence high quality factor. However, confining WGM modes in a circumference $2\pi R$ with R the resonator radius yields a mode spacing of $\Delta f = \frac{c_0}{\sqrt{\varepsilon_r}(2\pi R)}$, meeting the condition of an integer number of modes surrounding the resonator circumference, with $c_0 = 3 \cdot 10^8$ m/s the velocity of an electromagnetic wave in vacuum. Aiming at $\Delta f = 100$ MHz when using a relative permittivity material $\varepsilon_r = 40$, the resonator radius would be $R = 7.4$ cm. Fig. 5 reports the measurement of the frequency of a 3.4 cm-diameter WGM sapphire versus the resonator temperature using a wireless interrogation. The sapphire resonator is located in a metallic cavity to limit radiation losses. The sapphire resonator temperature can be varied thanks to an electronic temperature controller directly embedded on the cavity (Fig. 5, inset)[29]. A $WGH_{8,0,0}$ mode

at 9.51 GHz[30] is excited. The loaded quality factor is 80000. The minimum of the reflection coefficient is -4 dB. These correspond to an unloaded quality factor of 150000. The small resonator exhibits large mode spacing of 0.9 GHz due to the relatively low permittivity of sapphire: $\varepsilon_r \simeq 9$. Such a frequency separation is not compatible with a differential analysis which requires two modes to fit within the allocated band[7]. Fig. 5 reports the measurement of the sapphire resonator frequency versus temperature using a wireless interrogation. The temperature coefficient of frequency is measured to be -69 ppm/K, in very good agreement with values measured using a network analyzer and the literature[31].

[FIG. 5 about here.]

V. CONCLUSION

We have demonstrated the use of high quality microwave resonators as passive cooperative targets interrogated through a wireless link. The energy storage capability of the resonator is used to distinguish the delayed signal from the clutter generated by the wideband surrounding reflectors. Interrogation ranges above 1 m are thus achieved, and the resonance frequency is measured accurately enough to extract a temperature information remotely with a standard deviation of 3 K resolution.

ACKNOWLEDGEMENTS

We acknowledge V. Plessky (GVR, Switzerland), V. Giordano, Y. Kersalé and S. Grop (FEMTO-ST, Time & Frequency, Besançon, France) as well as H. Aubert (LAAS, Toulouse, France) for fruitful discussions. Y. Gruson (FEMTO-ST, time & frequency, Besançon, France) kindly provided the dielectric resonator and associated assembly setup.

SUPPLEMENTARY MATERIAL

Fig. 6 exhibits the experimental setup demonstrating the wireless interrogation of a dielectric resonator located 1 m away (left) from the microwave RADAR system (right). The red arrows on the oscilloscope screenshot are guides for the eye indicating the beat signal with the wave returned by the resonator.

[FIG. 6 about here.]

REFERENCES

[1]H. E. Stockman. Communications by means of reflected power. *Proceedings of the IRE*, 36(10):1196–1204, 1948.

[2]X Q. Bao, W. Burfhand an V.V. Varadan, and V.K. Varadan. SAW temperature sensor and remote reading system. In *IEEE Ultrasonics Symposium*, pages 583–585, 1987.

[3]F. Schmidt, O. Sczesny, L. Reindl, and V. Mhgori. Remote sensing of physical parameters by means of passive surface acoustic wave devices ("ID-TAGS"). In *IEEE Ultrasonics Symposium*, pages 589–592, 1994.

[4]W. Buff, F. Plath, 0. Schmeckebier, M. Rusko, T. Vandahl, H. Luck, F. Möller, and D.C. Malocha. Remote sensor system using passive SAW sensors. In *IEEE Ultrasonics Symposium*, pages 585–588, 1994.

[5]W. Buff, S. Klett, M. Rusko, J. Ehrenpfordt, and M. Goroli. Passive remote sensing for temperature and pressure using SAW resonator devices. *IEEE transactions on ultrasonics, ferroelectrics, and frequency control*, 45(5):1388–1392, september 1998.

[6]A. Pohl. A review of wireless SAW sensors. *IEEE transactions on ultrasonics, ferroelectrics, and frequency control*, 47(2):317–332, 2000.

[7]J.-M Friedt, C. Droit, G. Martin, and S. Ballandras. A wireless interrogation system exploiting narrowband acoustic resonator for remote physical quantity measurement. *Rev. Sci. Instrum.*, 81:014701, 2010.

[8]V. Plessky, Z.J. Davis, S. Suchkov, and M. Lamothe. 6 GHz SAW-tags and sensors. In *28th EFTF*, 2014.

[9]D. Morgan. *Surface Acoustic Wave Filters, 2nd Ed.* Academic Press, 2007.

[10]J Hoppe, J-M Boccard, T Aftab, A Yousaf, A Ojha, T Ostertag, and LM Reindl. Open parallel-plate dielectric resonator for passive torque sensing. In *Multi-Conference on Systems, Signals & Devices (SSD), 2014 11th International*, pages 1–5. IEEE, 2014.

[11]H. Cheng, S. Ebadi, and X. Gong. A low-profile wireless passive temperature sensor using resonator/antenna integration up to 1000^{o}C. *IEEE Antennas and Wireless Propagation Letters*, 11:369–372, 2012.

[12]X. Ren, S. Ebadi, Y. Chen, L. An, and X. Gong. Characterization of SiCN ceramic material dielectric properties at high temperatures for harsh environment sensing applications. *IEEE Transactions on Microwave Theory and Techniques*, 61(2):960–970, February 2013.

[13]A. Ojha, A. Yousaf, and L.M. Reindl. Characterization of dielectric resonator as a passive mechanical sensing element. In *Sixth International Conference on Sensing Technology (ICST)*, pages 219–225, 2012.

[14]A. Stelzer, S. Scheiblhofer, S. Schuster, and M. Brandl. Multi reader/multi-tag SAW RFID systems combining tagging, sensing, and ranging for industrial applications. In *Proc. IEEE IFCS*, Honolulu, HI, USA, 2008.

[15]G. Scholl, L. Reindl, W. Ruile, and T. Ostertag. Identification and/or sensor system, 1997. US Patent 5691698.

[16]H. Aubert, F. Chebila, M. Jatlaoui, T. Thai, H. Hallil, A. Traille, S. Bouaziz, A. Rifaï, P. Pons, P. Menini, and M. Tentzeris. Wireless sensing and identification based on radar cross section variability measurement of passive electromagnetic sensors. *annals of telecommunications*, 68(7-8), 2013.

[17]P. Pons, H. Aubert, P. Menini, and M. Tentzeris. Electromagnetic transduction for wireless passive sensors. *Procedia Engineering*, 47:1474–1483, 2012.

[18]T.T. Thai, J.M. Mehdi, F. Chebila, H. Aubert, P. Pons, G.R. DeJean, M.M. Tentzeris, and R. Plana. Design and development of a novel passive wireless ultrasensitive RF temperature transducer for remote sensing. *IEEE Sensor Journal*, 12(8):2756–2766, 2012.

[19]T.T Thai, F. Chebila, J.M Mehdi, P. Pons, H. Aubert, G.R DeJean, M.M Tentzeris, and R. Plana. A novel passive ultrasensitive RF temperature transducer for remote sensing and identification utilizing radar cross sections variability. In *Antennas and Propagation Society International Symposium (APSURSI), 2010 IEEE*, pages 1–4. IEEE, 2010.

[20]H. Aubert, F. Chebila, M.M. Jatlaoui, T. Thai, H. Hallil, A. Traille, S. Bouaziz, A. Rifai, P. Pons, P. Menini, and M. Tentzeris. Wireless sensing and identification of passive electromagnetic sensors based on millimetre-wave fmcw radar. *IEEE RFID Technology & Applications*, 2012.

[21]W. McC. Siebert. *Circuits, Signals, and Systems, 11th printing.* The MIT Press, 1998.

[22]D. Kajfez and P. Guillon. *Dielectric Resonators – 2nd Ed.* Nobleb Publishing Corporation, 1990.

[23]G.L. Charvat. *Small and Short-Range Radar Systems.* The MIT Press, 2014.

[24]S. Tourette, G. Collin, P. Le Thuc, C. Luxey, and R. Staraj. Small meandered PIFA associated with SAW passive sensor for monitoring inner temperature of a car exhaust header. In *IEEE International Workshop on Antenna Technology, iWAT*, pages 1–4, Santa Monica, CA, USA, 2009.

[25]J.-M Friedt, C. Droit, G. Martin, and S. Ballandras. A wireless interrogation system exploiting narrowband acoustic resonator for remote physical quantity measurement. *Rev. Sci. Instrum.*, 81:014701, 2010.

[26]B. Kubina, Martin Schüßler, C. Mandel, A. Mehmood, and R. Jakoby. Wireless high-temperature sensing with a chipless tag based on a dielectric resonator antenna. In *IEEE Sensors*, pages 1–4, Baltimore, MD, USA, 2013.

[27]X. Gong and L. An. Ceramic sensors for wireless high-temperature sensing, 2010. US Patent 0321191.

[28]M Hoft. New concepts for dielectric multi-mode resonators with branches. In *IEEE MTT-S International Microwave Symposium Digest*, pages 727–730, Atlanta, GA, USA, 2008.

[29]R. Boudot, C. Rocher, N. Bazin, S. Galliou, and V. Giordano. High-precision temperature stabilization for sapphire resonators in microwave oscillators. *Rev. Sci. Instrum.*, 76:095110, 2005.

[30]R. Boudot, Y. Gruson, N. Bazin, E. Rubiola, and V. Giordano. Design and measurement of low phase-noise x-band oscillator. *Electronics Letters*, 42(16):929–930, 2006.

[31]V.B. Braginsky, V.S.H. Chenko, and K.S. Bagdassarov. Experimental observation of fundamental microwave absorption in high quality dielectric crystal. *Physics Letters A*, 120(6):300–301, 1987.

LIST OF FIGURES

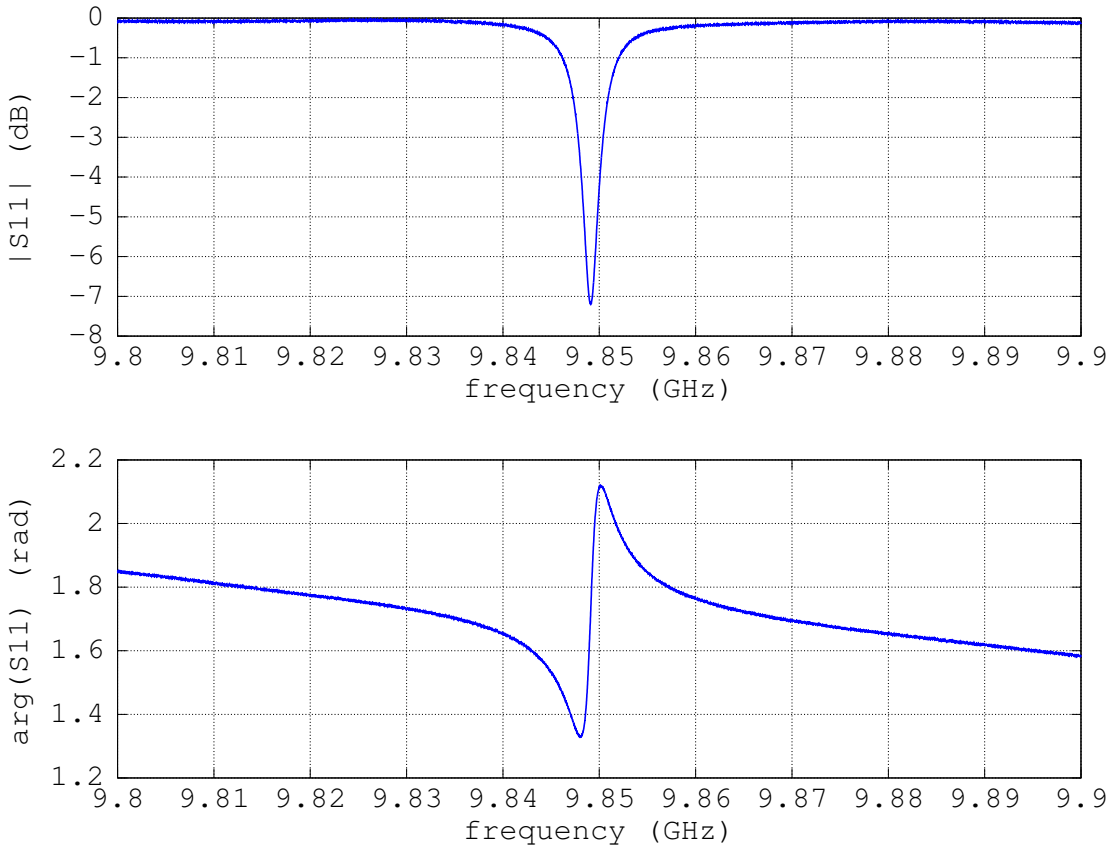

FIG. 1. Dielectric resonator reflection coefficient characterization (top: magnitude, bottom: phase).

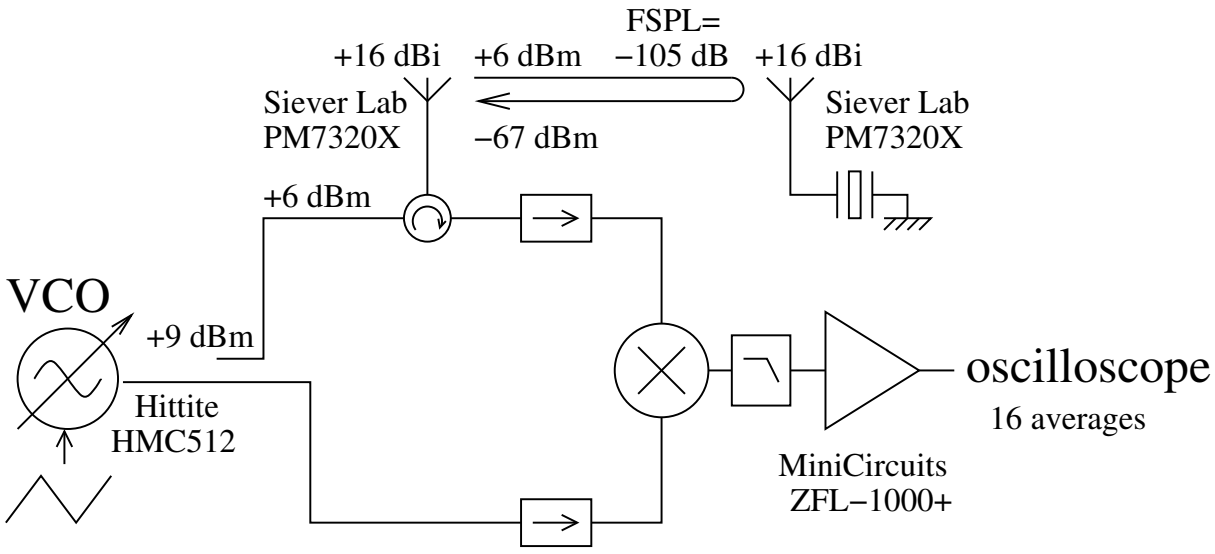

FIG. 2. Schematic of the interrogation circuit, including the link budget.

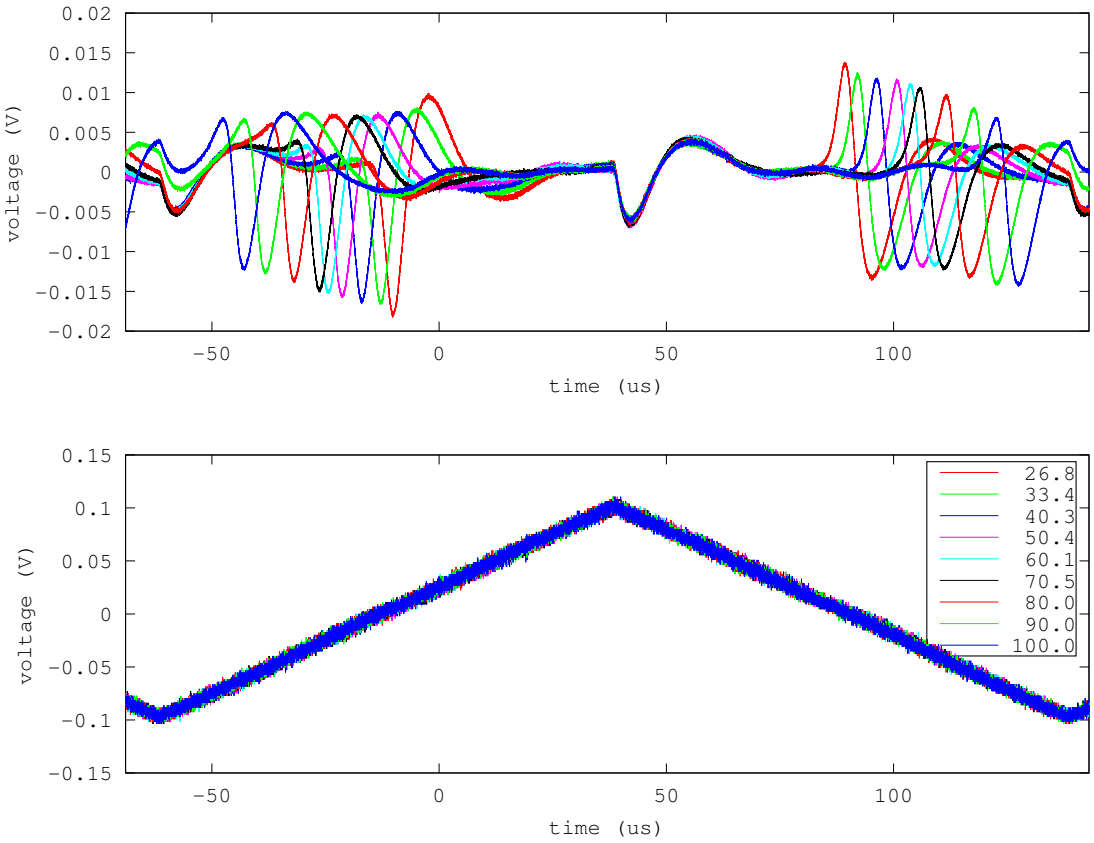

FIG. 3. Bottom: triangle shaped signal driving the VCO. The legend indicates the temperature at which each curve is recorded (in ^{o}C). Top: signal returned from the dielectric resonator as a function of temperature. The legend indicating the dielectric resonator temperature at which each curve was collected is valid for both graphs.

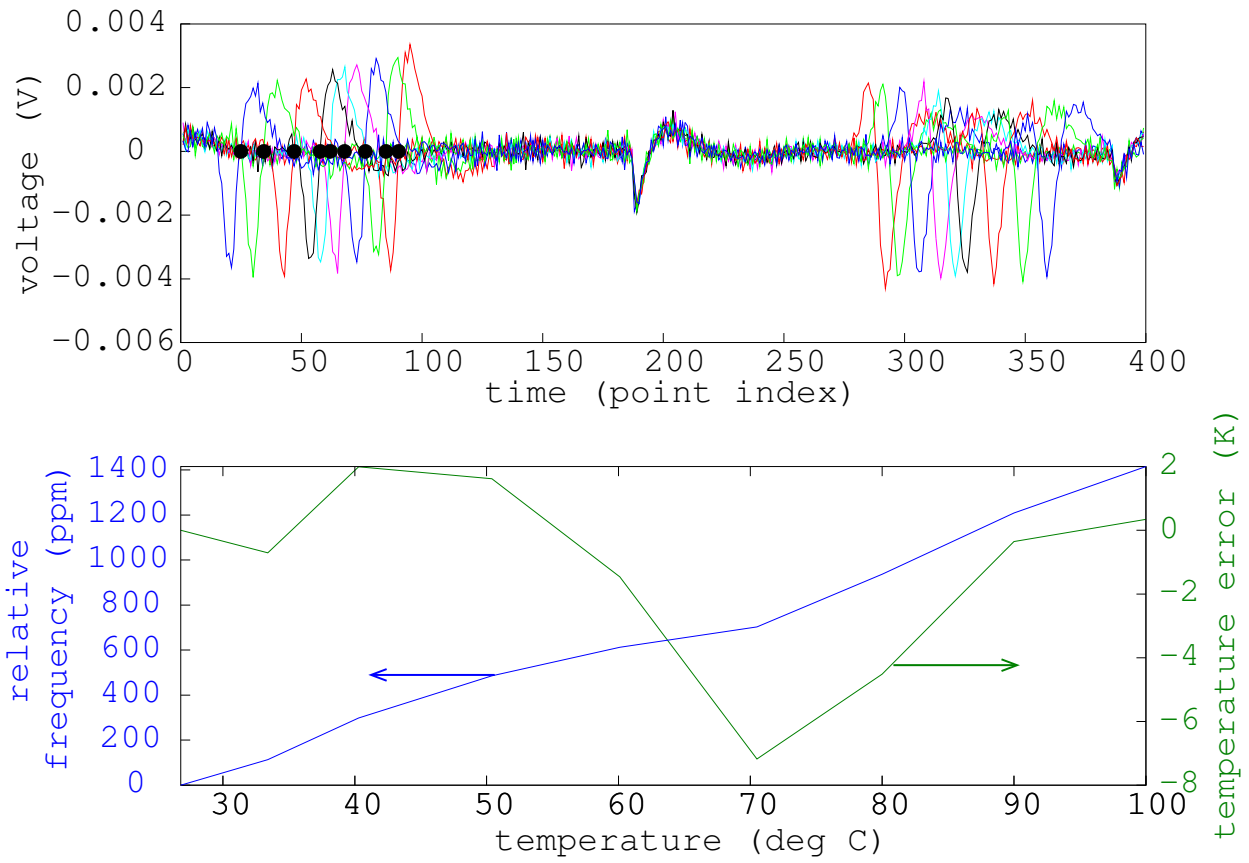

FIG. 4. Derivate of the returned signal for a precise identification of the resonance frequency (top): the time axis is provided in sample index to account for the oversampling when estimating the zero-crossing condition of the signal derivate (linear interpolation: the black circles indicate the zero crossing abscissa). Bottom: extracted temperature dependance of the dielectric resonator (left axis) with a first order coefficient resulting from a linear fit of the relative frequency dependence with temperature, and resulting measurement error (right axis) resulting from the subtraction of the estimated temperature and the measured outer resonator cavity temperature – the standard deviation of the measurement error (right-axis) is 3 K.

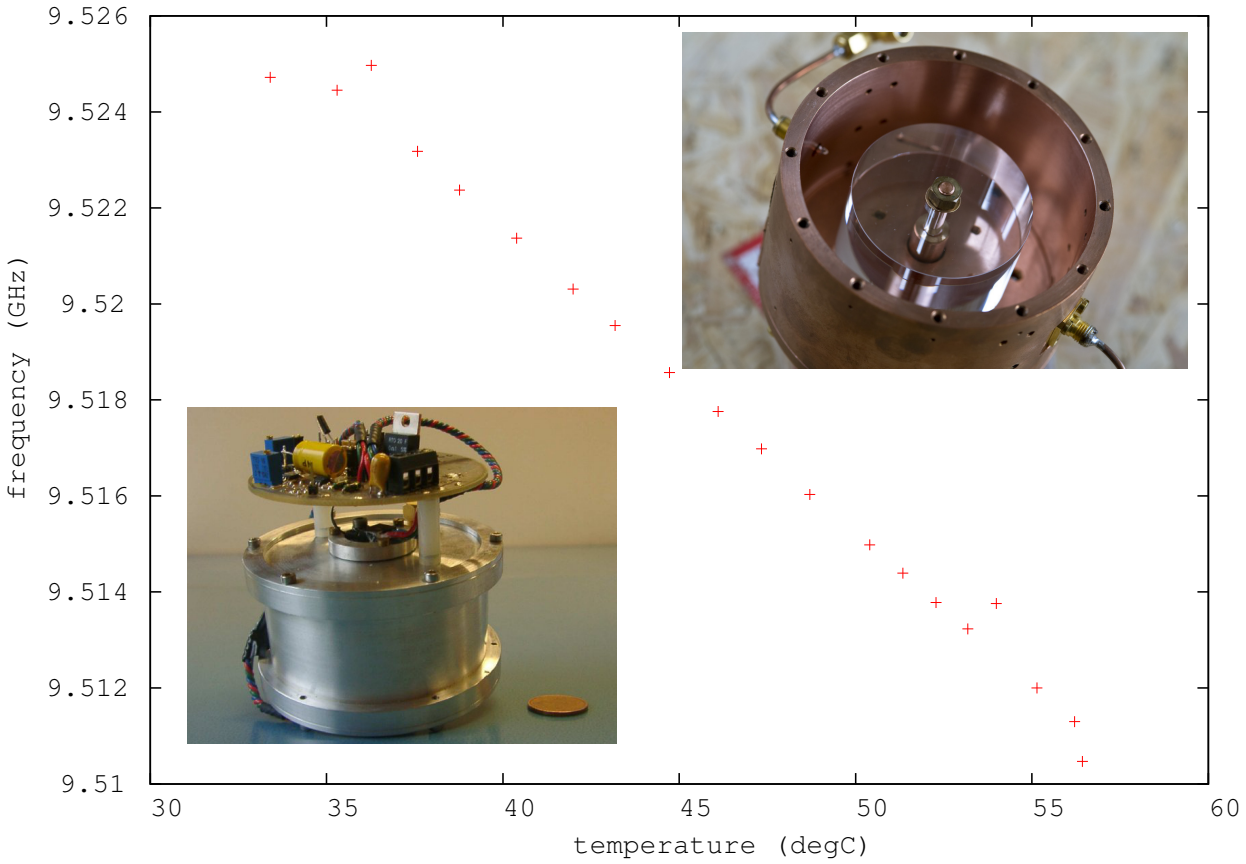

FIG. 5. Wireless characterization of a sapphire resonator resonance frequency temperature dependence, probed on the $WGH_{8,0,0}$ whispering gallery mode. Insets: pictures of the cavity containing the sapphire resonator (top right) and circuit for controlling the resonator temperature (bottom left).

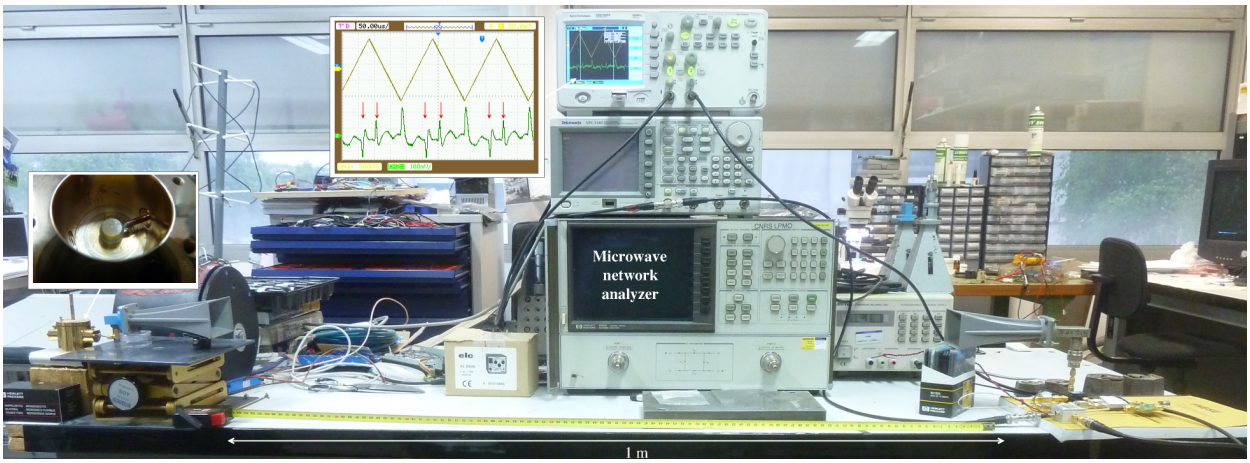

FIG. 6. Supplementary material: experimental setup demonstrating the interrogation range of over 1 m.